

Technical Notes

TECHNICAL NOTES are short manuscripts describing new developments or important results of a preliminary nature. These Notes should not exceed 2500 words (where a figure or table counts as 200 words). Following informal review by the Editors, they may be published within a few months of the date of receipt. Style requirements are the same as for regular contributions (see inside back cover).

Advanced Performance Simulation of a Turbofan Engine Intake

Vassilios Pachidis* and Pericles Pilidis†
Cranfield University,
Cranfield, England MK43 0AL, United Kingdom
Theodosios Alexander‡
Glasgow University,
Glasgow, Scotland G12 8QQ, United Kingdom
Anesths Kalfas§
Swiss Federal Institute of Technology,
8092 Zurich, Switzerland
and
Ioannis Templalexis¶
Hellenic Air Force Academy,
Dekeleia Air Base, TK 1010 Greece

Introduction

THE majority of today's engine simulation software is of a low fidelity (nondimensional). Such tools can offer a good prediction of the performance of a whole engine but are incapable of analyzing the performance of individual engine components in detail, or capturing extreme/complex physical phenomena, that is, inlet flow distortion. On the other hand, computational fluid dynamics (CFD) tools can predict the performance of individual engine components satisfactorily, especially close to design point (DP) operating conditions, but do not offer whole engine performance prediction.

Two issues prevent modeling the entire geometry of a propulsion system at the highest level of resolution (three dimensional) from being a practical solution. First, for a complete three-dimensional system simulation, the amount and level of detailed information needed as boundary and initial conditions would be extremely difficult to obtain. Second, the computational time and cost will be extremely high for effective and practical use.^{1,2}

Received 26 October 2004; revision received 18 August 2005; accepted for publication 24 August 2005. Copyright © 2005 by the American Institute of Aeronautics and Astronautics, Inc. All rights reserved. Copies of this paper may be made for personal or internal use, on condition that the copier pay the \$10.00 per-copy fee to the Copyright Clearance Center, Inc., 222 Rosewood Drive, Danvers, MA 01923; include the code 0748-4658/06 \$10.00 in correspondence with the CCC.

*Research Assistant, School of Engineering, Department of Power, Propulsion and Aerospace Engineering, Gas Turbine Engineering Group; v.pachidis@cranfield.ac.uk.

†Head, Gas Turbine Engineering Group, School of Engineering, Department of Power, Propulsion and Aerospace Engineering; p.pilidis@cranfield.ac.uk.

‡James Watt Professor, Department of Mechanical Engineering, Vanies Watt Building; t.alexander@mech.gla.ac.uk.

§University Lecturer, Department of Mechanical and Process Engineering—Institute of Energy Technology Turbomachinery Laboratory; kalfasa@asme.org.

¶Research Officer, Section of Thermodynamics, Power and Propulsion; templalexis@hafa.gr.

Scope of Work

Given the computational and financial resources of many industrial and academic establishments around the world, a fast method of combining different levels of analysis seems to be necessary. This study discusses two simulation strategies that allow the performance characteristics of an isolated gas turbine engine component, resolved from a detailed, high-fidelity analysis, to be transferred to an engine system analysis carried out at a lower level of resolution.

The techniques described in this Note are partially integrated zooming and fully integrated zooming. Both utilize an object-oriented, zero-dimensional gas turbine modeling and performance simulation system and a high-fidelity, three-dimensional CFD model of the intake of a modern high-bypass-ratio (HBR) turbofan engine. The first technique involves the generation of a component characteristic map via an iterative execution of the nondimensional cycle and the three-dimensional CFD model. The CFD-generated performance map can fully define the characteristic of the intake at several operating conditions and is subsequently used to provide a more accurate, physics-based estimate of intake performance, that is, pressure recovery, and, hence, engine performance, replacing the default, empirical values within the nondimensional cycle model. This work investigates relative changes in the simulated engine performance after integrating the CFD-generated component map into the nondimensional engine analysis. The analysis carried out by this study, demonstrates relative changes in the simulated engine performance larger than 1%.

The second technique is basically an extension of the first and adopts a more direct and fully automated approach with the three-dimensional CFD model being directly linked to the nondimensional engine cycle via the nondimensional component. The generation of a map in this case is not necessary. With the two methods being fairly similar in both execution and result, this Note discusses both of them, but focuses mainly on the first one, which is less straightforward.

Literature Review

Other research efforts with similar focus have been reported in the past. Turner et al.³ discussed a multifidelity simulation of a turbofan engine with component characteristics zoomed into partial performance maps for a nondimensional cycle simulation. AuBuchon and Follen¹ described a government–industry collaborative effort on one-dimensional compressor zooming. Yin^{4,5} has carried out significant research on an HBR two-dimensional fan zooming in the context of an academic project sponsored by industry. Reed and Afjeh^{6–8} have also published on numerical zooming techniques, in the context of the numerical propulsion system simulation (NPSS) program in 1997, Reed and Afjeh⁹ published a paper on a comparative study of high- and low-fidelity fan models for turbofan engine system simulation. Smith¹⁰ reported another collaborative research effort between the U.S. government and industry on fan and compressor high-fidelity zooming.

Simulation Strategy

Partially integrated zooming^{11,12} is a semimanual approach to high-fidelity analysis and can become fully automated as already mentioned. After the selection of engine operating conditions and power setting, a nondimensional engine model simulation is carried out to generate a first set of component operating conditions. The established component inlet/outlet boundary conditions from

the nondimensional cycle simulations are used to define component boundary conditions in the three-dimensional model simulation. Operating characteristics of the three-dimensional component model are then compared against the initial nondimensional solution.

Initially the nondimensional component will not match the high-fidelity component for various reasons such as: 1) the nondimensional component being of low fidelity, 2) geometry not taken into account in nondimensional simulations, 3) intercomponent effects not taken into account in the high-fidelity simulations, etc. Boundary conditions need to be updated and exchanged between the two component representations, in an iterative process, until a converged component performance is achieved at the given engine operating conditions and power setting.

If the nondimensional and three-dimensional flow solutions are in agreement, within a preestablished error margin, the averaged three-dimensional flow solution establishes a point on a component performance map to be used at a later stage for the whole engine performance simulation. If the flow solutions are not in agreement, the three-dimensional boundary conditions are communicated back to the nondimensional engine model as a second guess. The nondimensional engine model simulation is carried out again to provide new, updated boundary conditions for the three-dimensional CFD simulation. The process is repeated many times, until the two solutions agree within the preestablished error margin, then a new point on the component performance map is generated. Repeating the process for different engine operating conditions and power settings establishes the full-component performance map. The new, CFD-generated component map can be stored and used by the nondimensional cycle program in future engine simulations by employing common interpolation and scaling routines. The partially integrated zooming technique can be applied to all engine components that can be modeled in two or three-dimensions (Fig. 1).

The method just described can be extended to become fully integrated with the three-dimensional CFD component model being directly linked to the nondimensional engine model via the nondimensional component. Generation of a complete component characteristic map is not required in this case (Fig. 1).

The fully integrated strategy would perhaps be more appropriate for engine components such as intakes and ducts, where performance and boundary conditions do not change significantly offde-

sign. However, the performance and operating conditions of rotating components such as fans, compressors, and turbines change significantly offdesign. To reduce the computational demand, these components could be modeled adopting the partially integrated approach that reduces the number of CFD runs through the generation of a component characteristic.

Simulation Tools

Using the CFM56-5B2 HBR turbofan engine as a case study, this work looked into intake pressure recovery effects on whole engine performance, following the partially integrated described zooming approach.

The study used two different simulation software: 1) a nondimensional gas turbine modeling and performance simulation system, developed at Cranfield University in the United Kingdom, called PYTHIA^{13–15} and 2) the commercial CFD package GAMBIT/FLUENT.

For the purposes of this investigation, an engine model was build in PYTHIA that resembles the CFM56-5B2 HBR turbofan engine in both configuration and performance. The modeling was based on engine performance data available in the public domain.

Moreover, a three-dimensional CFD intake model, based on the geometry of the intake of the CFM56-5B2 HBR turbofan engine, was created and meshed in the commercial package GAMBIT using approximately 300,000 cells. The optimum number of cells was established by a grid-independence study. The commercial CFD solver, FLUENT, was used to carry out the CFD analysis. The geometry of the intake was similarly obtained from the public domain.

Typically, a PYTHIA engine model uses performance maps for turbines and compressors to obtain a balanced, steady-state engine condition. Intake pressure recovery is simplistically simulated by means of an empirical total pressure drop at both design point and offdesign conditions.

To establish the baseline intake and engine performances for the zooming analysis, the nondimensional intake characteristics were calibrated such that at the baseline conditions (DP) there was no difference between the nondimensional intake performance, that is, pressure recovery, mass flow, etc., and the performance predicted by the full, three-dimensional CFD intake model.

Intake Map Generation

Generating a point on the intake characteristic map involved the iterative process described in the “Simulation Strategy” section. Boundary conditions were exchanged between the two component representations until a converged component performance was achieved at the given engine operating conditions and power setting. A Newton–Raphson numerical method was used to control the convergence process.

The zooming analysis reported in this paper looked into different Mach numbers and operating altitudes for a fixed engine power setting and incidence angle. Varying altitude and Mach number gave a satisfactory range of different intake inlet operating conditions and a realistic, partial intake characteristic map for the selected power setting. More analytically, the engine’s power setting was kept at the DP value of 1458.15 K turbine entry temperature (TET) and incidence angle was kept at 0 deg. Points on the intake characteristic map were obtained for Mach numbers between 0.8 (DP value) and 0.3 and for a range of altitudes between 10,670 (DP value) and 2000 m (Fig. 2).

Repeating the process for different engine operating conditions, power settings, and incidence angles establishes the full-intake-performance map. At this stage, however, it was outside the scope and requirements of the investigation to repeat the same methodology for a larger number of different cases.

The CFD-generated map fully defined the performance characteristics of that particular intake geometry, at the simulated operating conditions, and was then used to provide a more accurate, physics-based estimate of the intake’s performance, that is, pressure recovery, and, hence, engine performance, replacing the empirical pressure recovery values within the PYTHIA cycle model.

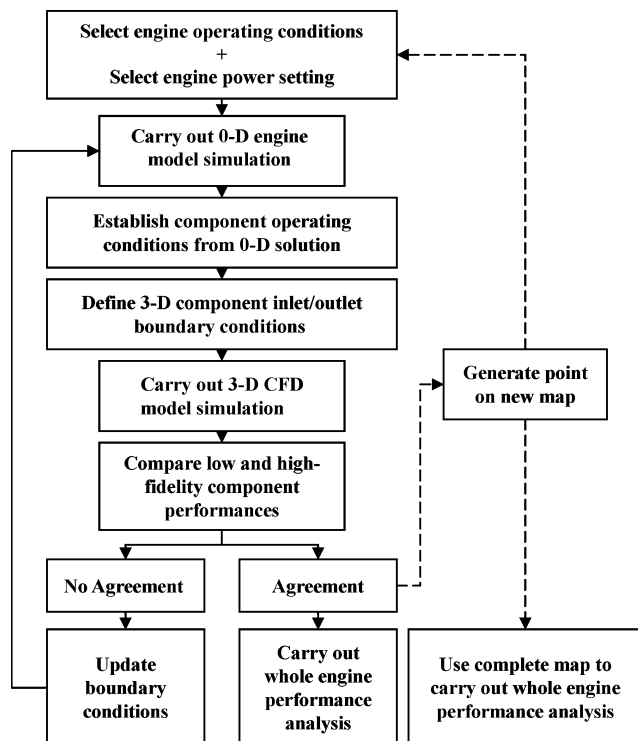


Fig. 1 Zooming strategies: ----, partially integrated and —, fully integrated.

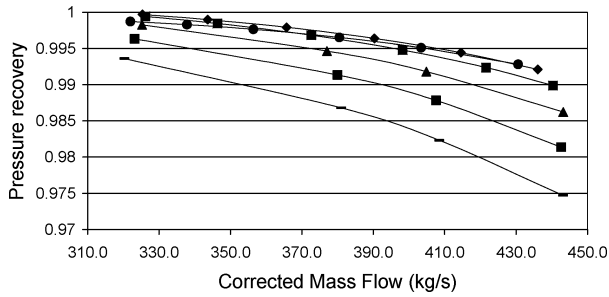


Fig. 2 CFD-generated partial intake characteristic: —, Mach number 0.3; —■, Mach number 0.4; —▲, Mach number 0.5; —■, Mach number 0.6; —◆, Mach number 0.7; and —●, Mach number 0.8.

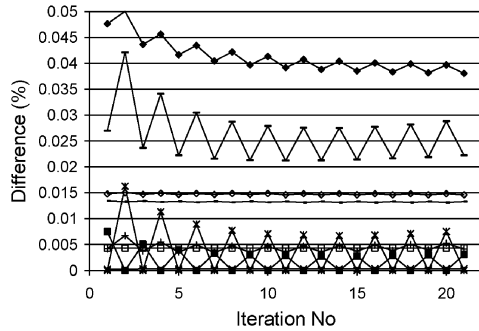


Fig. 3 Convergence history using a small flow domain: —■, V2; —◆, mass flow; —*, Pstat2; —+, Tstat2; —x, Ttot2; —, pressure recovery; —, Pstat1; —□, Tstat1; and —◇, V1.

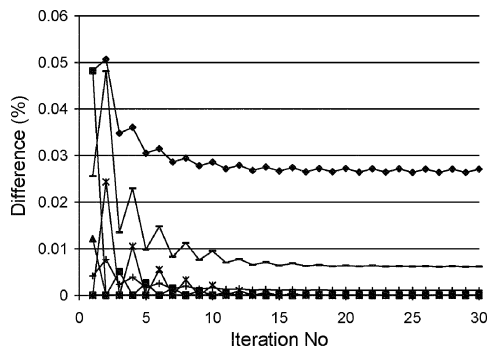


Fig. 4 Convergence history using bigger flow domain: —■, V2; —◆, mass flow; —*, Pstat2; —▲, Ptot2; —+, Tstat2; —□, Ttot2; and —, pressure recovery.

Convergence

As mentioned before, to generate a point on the map, matching the boundary conditions of the three-dimensional CFD intake model to those of the nondimensional intake component required an iterative execution of PYTHIA and FLUENT. Initial nondimensional cycle and three-dimensional CFD test runs, using a small, localized domain revealed a very poor convergence probability. Figures 3 and 4 show some convergence history samples of intake boundary conditions for PYTHIA–FLUENT iterative runs close to DP conditions.

On several occasions and particularly in those cases were extreme operating conditions were selected (resulting in unrealistic boundary conditions), the percentage difference between boundary conditions seemed to oscillate and/or even diverge. Figure 3 is representative of this sort of unstable iterative solution. In this particular case, most boundary condition differences seem to oscillate considerably around a certain percentage value with the pressure recovery difference oscillating around 2.5%, after 10 iterations, and then starting to diverge. The difference in mass flow is also fairly large, 3.7% approximately after 21 iterations. Iterating for other points on the characteristic map demonstrated similar unstable computational behavior.

Improving the CFD intake model (denser grid) and using a bigger flow domain, which also accounted for the flow outside the engine’s nacelle, seemed to improve the computational stability of the solution and the chances for convergence. Figure 4 is representative of this group of iterative runs between PYTHIA and FLUENT. The difference in mass flow reduced to approximately 2.7% after 15 iterations, whereas the difference in pressure recovery converged to a satisfactory 0.6%. All other boundary conditions converged to less than 0.25%.

Applying a correction factor to the outlet static pressure prediction of the nondimensional intake component, in every iteration, to take into account the presence of the fan and its effects on the flowfield improved the relatively large difference in mass flow even further and led to a much faster convergence. For this type of iterative run, all boundary conditions converged after three or four iterations within an acceptable 0.05%.

Engine Performance Simulation

Subsequent engine performance analysis demonstrated differences in the simulated engine performance between using the standard, empirical intake pressure recovery values and using the complete intake characteristic map. At cruise conditions and DP power setting, the simulation results, using the CFD-generated map, matched the baseline engine performance very well. As expected, only third-decimal-place differences were observed. The largest differences in engine performance were observed at operating conditions other than those at cruise (off-design conditions).

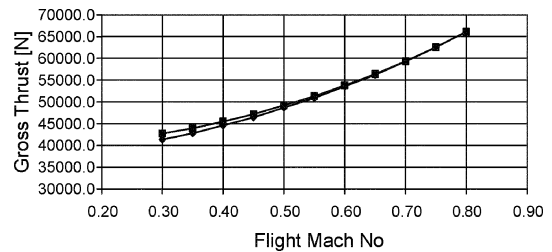


Fig. 5 Flight Mach number vs gross thrust, altitude = 10,670 m and TET = 1458.15 K: —◆, pressure recovery from map and —■, pressure recovery fixed at DP value.

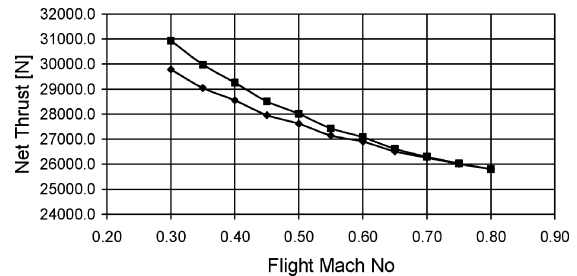


Fig. 6 Flight Mach number vs net thrust, altitude = 10,670 m and TET = 1458.15 K: —◆, pressure recovery from map and —■, pressure recovery fixed at DP value.

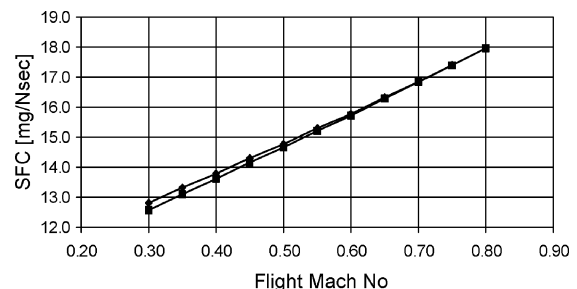


Fig. 7 Flight Mach number vs SFC, altitude = 10,670 m and TET = 1458.15 K: —◆, pressure recovery from map and —■, pressure recovery fixed at DP value.

Using the CFD-generated map and lowering the flight Mach number from 0.8 to 0.3 (maintaining DP altitude and power setting) gave a 3.3% reduction in engine gross thrust (at $M = 0.3$) compared to the baseline engine performance (empirical pressure recovery). Net thrust went down by approximately 3.9% and specific fuel consumption increased by 1.9% at $M = 0.3$. The engine performance at Mach number 0.8 remained unaffected as expected (DP). Figures 5–7 show the preceding observations.

Conclusions

Generating map points through this iterative process successfully depends strongly on the quality of the CFD model geometry, grid fidelity, and the soundness of the operating conditions selected. The CFD-generated component map can be stored and used by the nondimensional cycle program in future engine simulations by employing common interpolation and scaling routines.

The analysis was carried out only at zero incidence angle and a fixed power setting. When exactly the same simulation strategy is followed, other power settings and incidence angles can be included in the analysis, with the generation of more maps, for an even more realistic intake/engine performance prediction, especially under takeoff and landing conditions.

This paper presents a detailed comparison between the simulated, baseline engine performance and that obtained by using the CFD-generated intake map. Results presented are to be taken only qualitatively because of the inherent uncertain accuracy of public domain data. However, in the cases examined, the analysis carried out by this study demonstrated relative changes in the simulated engine performance larger than 1%, which justifies the extra time that is usually required to create and run a three-dimensional CFD engine component, especially in those cases where more accurate, high-fidelity engine performance simulation is required.

References

¹AuBuchon, M., and Follen, G., "Numerical Zooming Between a NPSS Engine System Simulation and a One-Dimensional High Compressor Analysis Code," Computational Aerosciences Workshop, High Performance Computing and Communications Program, NASA TM-2000-209913, Feb. 2000.

²Evans, A., Follen, G., Naiman, C., and Lopez, I., "Numerical Propulsion System Simulation's National Cycle Program," AIAA Paper 98-3113, July 1998.

³Turner, M. G., Reed, J. A., Ryder, R., and Veres, J. P., "Multi-Fidelity Simulation of a Turbofan Engine with Results Zoomed into Mini-Maps for a Zero-D Cycle Simulation," *Proceedings of ASME Turbo Expo 2004*, GT2004-53956, American Society of Mechanical Engineers, 2004.

⁴Yin, J., "High Bypass Ratio Fan Modelling," Performance Engineering Rolls-Royce Univ. Technology Center Annual Review Rept., WP2, Cranfield Univ., Cranfield, England, U.K., March 1999.

⁵Yin, J., "Proposed Calculation Procedures for the Generation and Application of 2-D Fan Characteristics," Performance Engineering Rolls-Royce Univ. Technology Centre Document PE005, Ver. 2, School of Mechanical Engineering, Cranfield Univ., Cranfield, England, U.K., Aug. 1999.

⁶Reed, J. A., and Afjeh, A. A., "Development of an Interactive Graphical Propulsion System Simulator," AIAA Paper 94-3216, June 1994.

⁷Reed, J. A., and Afjeh, A. A., "Distributed and Parallel Programming in Support of Zooming in Numerical Propulsion System Simulation," *Proceeding of Symposium on Applications of Parallel and Distributed Computing*, 1994.

⁸Reed, J. A., and Afjeh, A. A., "An Interactive Graphical System for Engine Component Zooming in a Numerical Propulsion System Simulation," AIAA Paper 95-0118, Jan. 1995.

⁹Reed, J. A., and Afjeh, A. A., "A Comparative Study of High and Low Fidelity Fan Models for Turbofan Engine System Simulation," *Proceeding of the IASTED International Conference on Applied Modelling and Simulation*, July 1997.

¹⁰Smith, L. H., "NASA/GE Fan and Compressor Research Accomplishments," *Journal of Turbomachinery*, Vol. 116, No. 4, 1994, pp. 554–568.

¹¹Guideuil, G., Pachidis, V., and Pilidis, P., "Iterative Approach to 2D Component Zooming Applied to a Turbofan Intake," Technical Rept., School of Engineering, Dept. of Power, Propulsion and Aerospace Engineering, Gas Turbine Performance Group, Cranfield Univ., Cranfield, England, U.K., July 2004.

¹²Talhouarn, F., Pachidis, V., and Pilidis, P., "Partially Integrated Approach to 3-D Component Zooming Applied to the Intake," Technical Rept., School of Engineering, Dept. of Power, Propulsion and Aerospace Engineering, Gas Turbine Performance Group, Cranfield Univ., Cranfield, England, U.K., July 2004.

¹³Pachidis, V., "Gas Turbine Simulation—PYTHIA Workshop Guide," Pt. 1, *American Society of Mechanical Engineers/International Gas Turbine Institute Aero Engine Life Management Conference*, March 2004.

¹⁴Pachidis, V., "Gas Turbine Simulation—PYTHIA Workshop Guide," Pt. 2, *American Society of Mechanical Engineers/International Gas Turbine Institute Aero Engine Life Management Conference*, March 2004.

¹⁵Palmer, J. R., "The TURBOMATCH Scheme for Aero/Industrial Gas Turbine Engine Design Point/Off Design Performance Calculation," School of Mechanical Engineering, Thermal Power Group, Cranfield Univ., Cranfield, England, U.K., 1990.